JOURNAL OF Materials CHEMISTRY

Laser photolysis of liquid hexafluorobenzene: graphitic and fluorine-containing carbon formation at ambient temperature

Josef Pola,*[a] **Markéta Urbanová,**[a] **Zdeněk Bastl,**[b] **Zbyněk Plzák,**[c] **Jan Šubrt,**[c] **Ivan Gregora**[d] **and Vladimír Vorlíček**[d]

[a]*Institute of Chemical Process Fundamentals, 165 02 Prague*
[b]*J. Heyrovský Institute of Physical Chemistry 182 23 Prague*
[c]*Institute of Inorganic Chemistry, 250 68 Řež near Prague*
[d]*Institute of Physics, 180 40 Prague; Academy of Sciences of the Czech Republic, Czech Republic*

ArF laser photolysis of liquid hexafluorobenzene affords a number of aromatic fluorocarbons, graphitic carbon and a fluorine containing polymeric C/F material. The preponderance of decafluorobiphenyl among the perfluoroaromatic products reveals the importance of the pentafluorophenyl radical combinations in the initial stages of photolysis. The C/F material is judged to arise from polymerization of fluoroalkyne transients. The graphite formation represents a unique mode of photolytic liquid-phase graphitization of perfluoroaromatic compounds.

Pyrolytic carbon produced from organic compounds has received great interest. However, its photolytic counterpart and its formation from hydrocarbons in the liquid phase, which is now feasible through the use of the intense radiation of lasers, has hitherto been given only very little attention.

Lamp-induced photochemistry in the condensed phase of benzene and other unsubstituted aromatic molecules takes place only with low quantum efficiencies as ring isomerization,[1,2] however, irradiation of liquid benzene with intense laser pulses induces more dramatic changes. Thus, laser photolysis at 248 nm of aromatic compounds dissolved in cyclohexane results in a proton transfer from an excited aromatic radical cation,[3,4] and laser irradiation at 248 and 308 nm of neat benzene leads to liquid ablation and yields carbon and a multitude of aromatic compounds.[5] The latter process has been inferred to occur by a photochemical and not photothermal fragmentation.[6] A complete degradation into carbon has also been observed in 308 nm irradiation of a copper substrate immersed in liquid benzene[7] in which diamond films were inferred to be formed as a result of rapid quenching from high temperature.

In our preceding paper we described that ArF laser photolysis of liquid benzene and toluene affords polyaromatic hydrocarbons, graphite and polymeric carbon.[8] The remarkable feature of this process is that the graphite formation occurs at ambient temperature. The laser photolytic graphitization modes are therefore different from those involved in thermally induced graphitization taking place at temperatures above 2000 °C (ref. 9–11).

Here, we report on ArF laser photolysis of liquid hexafluorobenzene and explain it by a dominance of two reactions schemes, one leading to graphite and another to C/F material. The graphite formation occurring at ambient temperature of the irradiated liquid represents a unique mode of photolytic liquid-phase graphitization of perfluoroaromatic compound.

Experimental

Samples of freshly distilled hexafluorobenzene (Imperial Smelting) were contained in a 4 ml brass photolytic cell equipped with two fused quartz plates (effective diameter 0.8 cm) and were irradiated for 40 min by the unfocussed beam from an ArF excimer (model ELI 94) laser, operating at 193 nm with repetition frequency 10 Hz and energy fluence of 100 mJ cm^{-2}. In order to be able to record the FTIR spectra of volatile products, the photolytic cell was connected to a 10 cm long glass tube furnished with a stopcock and NaCl windows.

The irradiated liquid samples from which solid black particles were removed on a centrifuge, were concentrated by removing hexafluorobenzene by distillation and analysed on a Magnum GC–MS ion trap system (Finnigan MAT, USA). The system utilized a Varian SPI injector (held at 250 °C) and a DB-5ms capillary column (JW Scientific, USA) 30.0 m × 0.25 mm with 0.25 mm thickness. The carrier gas (He 99.996%) velocity was 33.1 cm s^{-1} (at 60 °C). The GC oven was maintained at 50 °C for 2 min, increased at 8 °C min^{-1} to a maximum 280 °C. Samples were introduced with a Hamilton syringe. The transfer line was held at 280 °C and ion manifold at 200 °C. For chemical ionization experiments methane and acetonitrile were used as reaction gases.[12] The ion trap was tuned using default software setting (Magnum 2.4., Finnigan MAT) to obtain suitable mass calibration, filament emission current, multiplier voltage and AGC (automatic gain control) settings.

Identification of individual organic compounds was based on comparison of their electron impact mass spectra with those of authentic compounds of the reference NIST library (National Institute of Standards and Technology Mass Spectrometry Library, 1990 Edition) and data published in ref. 13–16. Relatively a small number of perfluorocompounds have been included in these sources. Therefore, a tentative assignment of individual peaks in the chromatogram was mostly based on spectral interpretation of both electron impact and chemical ionization spectra.

Black particles centrifuged from the solution and washed in hexane formed thin films when their hexane suspensions were dropped on metal sheets kept at 60 °C. These films were analysed by Raman spectroscopy, XPS and also by SEM and TEM methods.

The photoelectron and Auger spectra were recorded in a VG ESCA 3 Mk II electron spectrometer. The background pressure during the spectra accumulation was in the 10^{-6} Pa range. The measurements were performed using an Al Kα ($h\nu = 1486.6$ eV) source at a power of 220 W. The spectrometer was operated in the fixed analyser transmission mode with a pass energy of 20 eV, giving a resolution of 1.1 eV on the Au ($4f_{7/2}$) line. The samples were spread on copper plates which were mounted on a sample probe by means of tantalum clips. The spectra of C 1s, O 1s, F 1s photoelectrons and the X-ray excited C KLL and F KLL Auger electrons were recorded. Curve fitting of high resolution spectra was accomplished using the Gaussian–Lorentzian lineshape and damped non-linear least squares procedure.[17] Photoelectron peak area computation was performed after the nonlinear background[18] was removed. Quantification of the surface concentrations of elements was accomplished by correcting the photoelectron peak areas for their cross-sections.[19]

Raman spectra of black particles were measured at room temperature. The exciting beam from an Ar-ion laser (514.5 nm) impinged the sample surface under the near-Brewster angle. To diminish the heating of the sample, the beam was slightly defocused and its incident power was kept below 30 mW. The PC-controlled spectrometer was coupled with a photomultiplier operating in the photon counting mode.

Scanning electron microscopy examination of the black particles deposited on Cu substrates was performed on an ultra-high vacuum Tesla BS 350 instrument equipped with an energy dispersive analyzer of X-ray radiation, EDAX 9100/65.

Transmission electron microscopy measurements of the black particles were carried out on a Philips 201 microscope.

Results and Discussion

ArF laser (193 nm) irradiation of liquid hexafluorobenzene results in an initially yellow and later black colouration of the liquid, which is caused by formation of a multitude of aromatic fluorocarbons and copious amounts of black particles composed of a graphitic and fluoropolymeric carbon.

Soluble aromatic products

GC–MS analysis of the liquid portion (Fig. 1) reveals that a very major component in the photolysis of hexafluorobenzene is decafluorobiphenyl, and that other aromatic products such as C_6F_8 and $C_{12}F_{12}$ fluorocarbons, octafluoroindene, perfluorodiphenylmethane, perfluoronaphthalene and perfluoroterphenyls are produced in significantly lower yields. There are still many other small peaks in the GC–MS trace. Regrettably, insufficient literature data on mass fragmentation of fluoroaromatic compounds make their assignment rather difficult. In discussing possible reaction steps occurring during the 193 nm liquid-phase photolysis of hexafluorobenzene, we are helped by the earlier reported photolysis of hexafluorobenzene in the gas phase. The mercury lamp-induced photoisomerization of hexafluorobenzene leads exclusively to hexafluorobicyclo[2.2.0]hexa-2,5-diene (hexafluoro-Dewar-benzene)[20,21] and the dye laser irradiation of hexafluorobenzene at collision-free conditions results in multiphoton fragmentation of hexafluorobenzene and formation of neutral carbon atoms as end products.[22]

The energy delivered by the single photon at 193 nm corresponds to *ca.* 620 kJ mol^{-1} which is enough to homolytically cleave both C–F bonds [for C_6F_6 estimated as 477 (ref. 23) or 644 (ref. 24–26) kJ mol^{-1}] and C—C bonds. Several decomposition pathways can be opened and those of lowest $\Delta H°$ ($\leqslant$502 kJ mol^{-1}) (ref. 27) given in eqn. (1)–(3), involve formation of fluorine atom together with pentafluorophenyl radical (1), cleavage into an unsaturated biradical (2), and *m*-fluorine migration coupled with retro-Diels–Alder decomposition affording tetrafluoroethene along with 1,4-difluorobuta-1,3-diyne (3).

$$C_6F_6 \rightarrow C_6F_5{}^{\bullet} + F^{\bullet} \qquad (1)$$

$$\rightarrow {}^{\bullet}FC{=}CF{-}CF{=}CF{-}CF{=}CF^{\bullet} \qquad (2)$$

$$\rightarrow FC{\equiv}C{-}C{\equiv}CF + F_2C{=}CF_2 \qquad (3)$$

The occurrence of the initial steps (1) and (2) is confirmed by the observed products; thus decafluorobiphenyl can only arise *via* the recombination of C_6F_5 radicals and it gives support to the pathway (1), and perfluorohexadiene can be produced by a reaction of fluorine with the 1,6-C_6F_6 biradical in the reaction (2). Fluorine produced in reaction (1) is consumed in formation of the observed C_6F_8 fluorocarbons. These fluorocarbons are apparently produced by a reaction of fluorine with intermediary hexafluoro-Dewar-benzene. Hexafluoro-Dewar-benzene dimerizations and rearrangements apparently afford the observed $C_{12}F_{12}$ products. The initial step (3) is not similarly supported. Fluorinated alkynes are very unstable due to spontaneous exothermic polymerization and escape observation (see *e.g.* ref. 28).

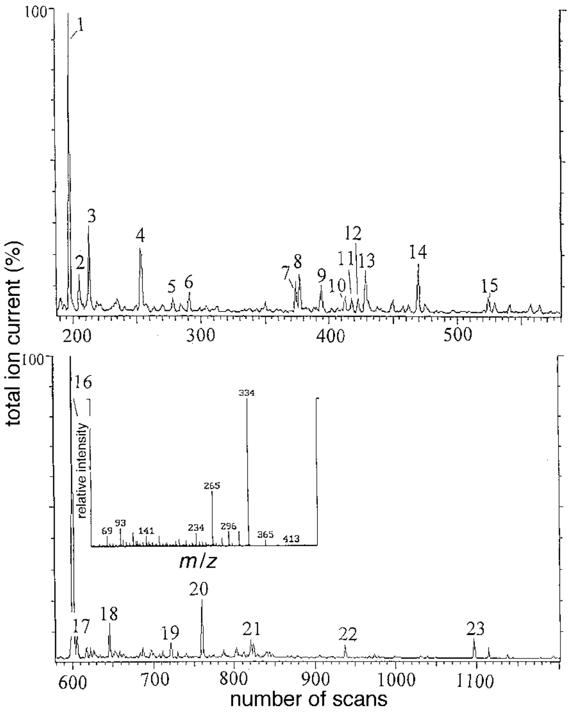

Fig. 1 Total ion current mass chromatogram of reaction mixture formed upon laser photolysis of hexafluorobenzene. Peak no., compound (percent of total area): 1, perfluorocyclohexadiene (9.5); 2, octafluoroindene (1.6); 3–5, C_6F_8 (2.8, 0.6 and 0.8, respectively); 6, trifluorobenzene (0.8); 7–14, $C_{12}F_{12}$ (1.1, 1.5, 1.3, 0.6, 0.6, 0.6, 2.4 and 2.0, respectively); 15, perfluorodiphenylmethane (0.7); 16, decafluorobiphenyl (61.6); 17, perfluoronaphthalene (1.2); 18, nonafluorobiphenyl (1.4); 19–21, $C_{12}F_{12}$ (0.8, 3.0 and 0.9, respectively); 22, *m*-perfluoroterphenyl (0.6); 23, *p*-perfluoroterphenyl (1.0).

Other possible routes can be those shown in eqn. (4)–(8).

$$C_6F_6 \rightarrow F_nC{:} + F^{\bullet} + \text{residue} \qquad (4)$$

$$F_2C + nF \rightarrow CF_{n+2} \qquad (5)$$

$$2CF_3 \rightarrow C_2F_6 \qquad (6)$$

$$2F_2C \rightarrow C_2F_4 \qquad (7)$$

$$2CF \rightarrow C_2F_2 \qquad (8)$$

$$(n = 1,2)$$

We did not observe formation of any gaseous product (CF_4, C_2F_4, C_2F_6), but believe that the CF_n transients ($n = 1,2$) are involved; thus perfluorodiphenylmethane can only be produced by reaction of F_2C: with C_6F_5 radicals, and trifluorobenzene is obviously formed by trimerization of HFC: originated from a reaction of CF with H-containing trace impurities or ambient atmosphere. (We note that the sample of C_6F_6 was not degassed prior to irradiation.) Similar reactions are obviously responsible for formation of pentafluorobenzene and nonafluorobiphenyl, and they indicate an occurrence of C_6F_5 and $C_6F_5{-}C_6F_4{}^{\bullet}$ radicals. We note that $C_6F_5{}^{\bullet}$, F_2C: and ${}^{\bullet}CF$:

species were found in the IR laser-induced decomposition of hexafluorobenzene.[29,30] The absence of the gaseous CF_4, C_2F_4, C_2F_6 products under our conditions thus reveals that the presumed F_2C: and $^{\bullet}CF$: transients undergo exclusively reactions yielding high-molecular compounds. These reactions must be faster than F_2C: self-recombination into C_2F_4, or recombination of $F^{\bullet}$ and F_2C: into CF_3 or CF_4.

Insoluble black particles

Properties of the black particles are revealed by Raman as well as photoelectron and Auger spectra. The spectrum of C 1s electrons (Fig. 2) is compared to that of graphite and that of particles produced by the ArF laser photolysis of benzene.[8] It is seen that the major constituent in both kinds of particles is elemental carbon. The observed overall stoichiometry for the particles produced from C_6F_6 is $C_{1.0}F_{0.29}O_{0.10}$, but the particles formed from C_6H_6 are almost entirely pure carbon [O/C = *ca.* 10^{-2} (ref. 8)]. Table 1 summarizes the measured core level binding energies of the fitted spectral lines along with the assignment based on the comparison of measured binding energies to the available literature data.[31–33] We have attempted to estimate the hybridization of carbon atoms using the energy difference between the most positive and most negative excursions of C KLL derivative spectra[34,35] (see Fig. 3). Similar energy differences, *ca.* 19 eV, are obtained for both samples which correspond to the presence of *ca.* 60% of sp^2 hybridized C atoms. We note that this value for the deposit from C_6F_6 is less accurate due to the complexity of the Auger spectrum caused by the non-negligible contribution of carbon atoms bonded to fluorine.

The formation of the C/F material can be explained by polymerization of the CF_n transients and of fluoroalkynes (difluoroethyne or 1,4-difluorobuta-1,3-diyne). The latter compounds polymerise spontaneously at low pressure in the gas phase[28] and would do so even more efficiently when produced in relatively high concentrations in the liquid phase.

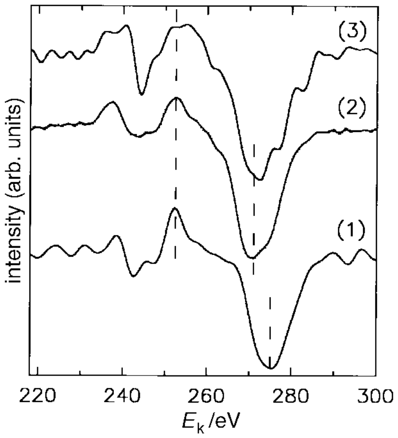

Fig. 3 C KLL derivative Auger spectra of (1) graphite, (2) black particles from ArF laser photolysis of benzene[8] and (3) black particles from ArF laser photolysis of hexafluorobenzene

The Raman spectrum in the range of 200–2000 cm^{-1} is dominated by a broad doublet between 1300–1600 cm^{-1} which is characteristic of the disordered graphitic type carbon (Fig. 4). Like in carbon-based films of various sorts,[36] this doublet can be decomposed into two Lorentzians peaking at 1370 and 1603 cm^{-1}. However, a much better fit is obtained with three Lorentzians at 1346, 1610 and 1538 cm^{-1} (Fig. 5). The first two components may be identified as the G and D bands

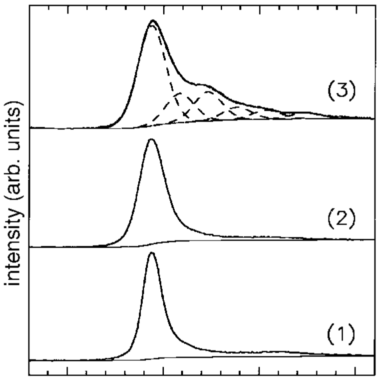

Fig. 2 C 1s core level spectra of (1) graphite, (2) black particles from ArF laser photolysis of benzene[8] and (3) black particles from ArF laser photolysis of hexafluorobenzene. The spectra are normalized to the same height.

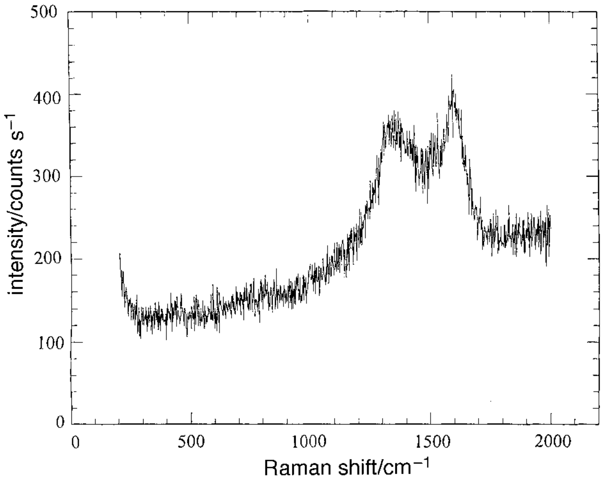

Fig. 4 Raman spectrum of the black particles from ArF laser photolysis of hexafluorobenzene (514.5 nm, 30 mW)

Table 1 Core level binding energies (E_b), population of individual chemical states (%) of elements and their assignment

precursor	line	E_b/eV	population	assignment
C_6H_6	C 1s	284.4	100	elemental carbon
C_6F_6	C 1s	284.4	53	elemental carbon
		285.8	15	$-\mathrm{CH_2}\mathit{C}\mathrm{HFCH_2}-$
		287.3	15	$-\mathit{C}\mathrm{HF{-}CH_2}-$; $-\mathrm{CO}-$
		288.8	7	$-\mathit{C}\mathrm{HFCHF}-$
		290.4	5	$-\mathit{C}\mathrm{F_2CH_2}-$
		292.4	3	$-\mathit{C}\mathrm{F_2CF_2}-$
	O 1s	531.9	78	$-\mathrm{CO}-$
		533.8	22	$-\mathrm{CH_2OH}$
	F 1s	687.4	100	
	F KLL	799.2[a]	100	

[a] Kinetic energy of KLL Auger electrons.

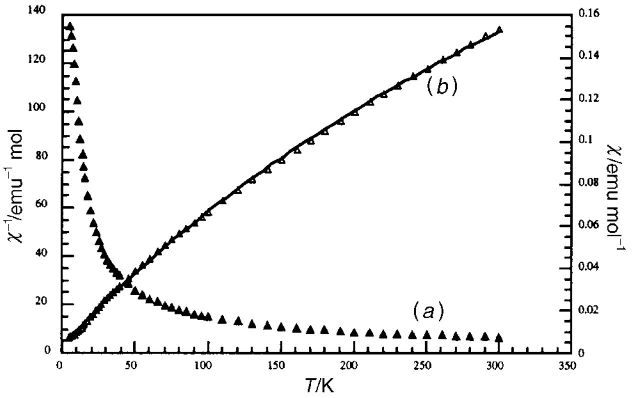

Fig. 5 Deconvolution of the dominating band of the Raman spectrum

typical of disordered graphite, the wavenumber of the third one falls into the region where, typically, the main peak of a-C (DLC) is observed.[36] A slight time decay of the signal, which we observed, is resembling the behaviour of the mixture of polymeric and graphitic carbon obtained from the liquid phase photolysis of benzene and toluene,[8] and it is due to a polymeric carbon which is known to show intense luminescence.[37] We believe that the incident light induces some changes of the polymeric component, leaving the graphitic carbon unchanged. The Raman spectrum does not show any feature proving the presence of F atoms. Similar absence of signals of an F—C framework was also reported in ref. 38.

The presence of F in the black particles is also detected by EDX–SEM analysis; the SEM micrograph of the black particles deposited on the Cu substrate reveals a continuous structure with some cracks (Fig. 6). Transmission electron microscopy of the particles reveals that their size is *ca.* 50 nm or more, and that these particles are aggregated to larger bodies (Fig. 7).

Although the lamp photolysis of benzene and hexafluorobenzene yields different products,[2] the former preferring fulvene and the latter hexafluorobicyclo[2.2.0]hexa-2,5-diene, the similarity of some final products from the ArF laser photolysis of hexafluorobenzene (octafluoroindene, perfluorodiphenylmethane, perfluoronaphthalene and perfluoroterphenyls) and of benzene (indene, diphenylmethane, naphthalene, and terphenyls, ref. 8) suggests that these polyaromatic fluorocarbons and hydrocarbons are produced by sequences of similar steps, and furthermore that the laser-photolytic formation of graphite from benzene and hexafluorobenzene, and also formation of polymeric C/H carbon from benzene and that of the C/F material from hexafluorobenzene, may also consist of common steps. We remark that possibly analogous steps involving C—C and C—F bonds during the laser photolysis of hexafluorobenzene, and C—C and C—H bonds during the laser photolysis of benzene,[8] must differ from those involved in thermally induced graphitization (ref. 9–11) which takes place at temperatures above 2500 °C. The incorporation of the significant amounts of oxygen and hydrogen into the black particles produced from C_6F_6 does not have parallel in the ArF laser photolysis of C_6H_6 (ref. 8) and it suggests that, apart from some common steps, laser photolysis of benzene and hexafluorobenzene show some differences possibly due to different reactivity of some intermediates and/or naked centers in growing agglomerates.

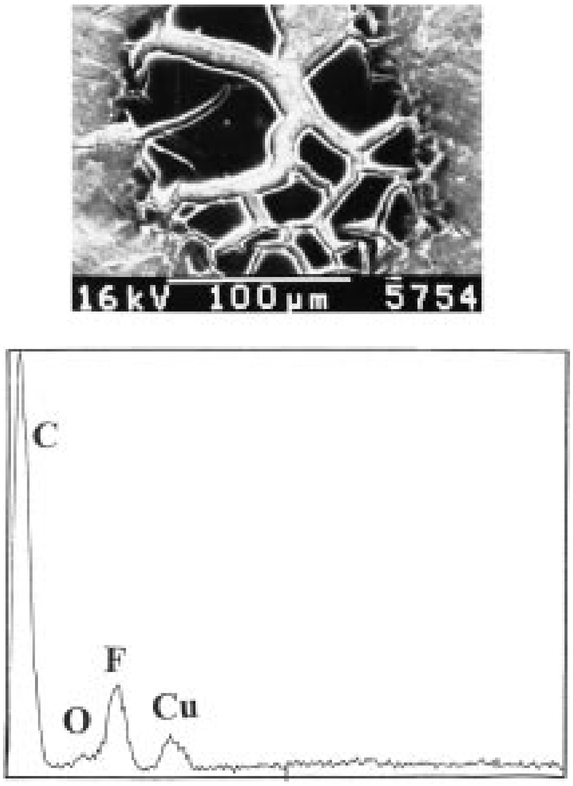

Fig. 6 SEM and EDX–SEM analysis of the black particles from ArF laser photolysis of hexafluorobenzene

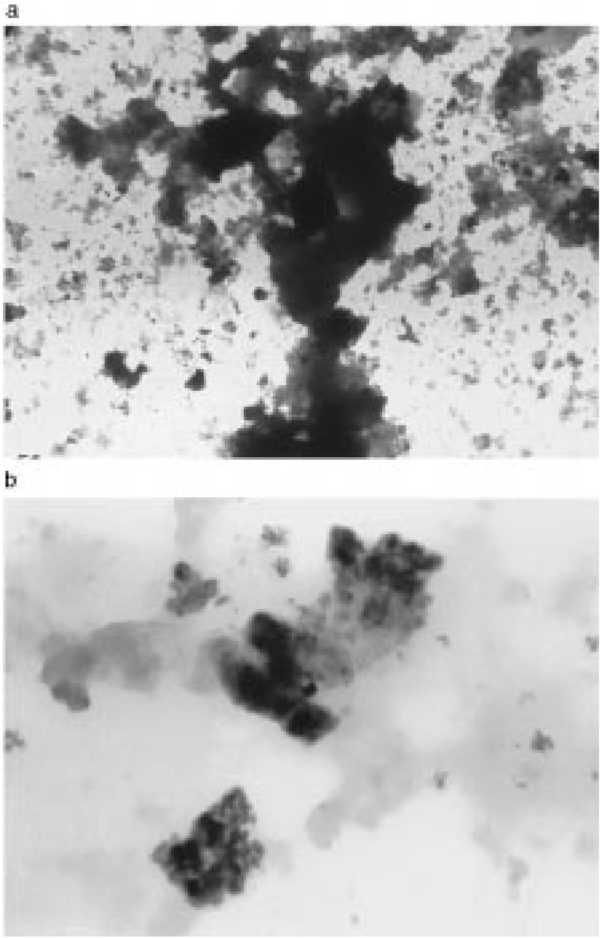

Fig. 7 TEM images of the black particles from ArF laser photolysis of hexafluorobenzene. Magnification 10 000 (a) and 100 000 (b).

This work was supported by the NATO Scientific Affairs Division and the Ministry of Education, Youth and Sports of the Czech Republic [grant no. ES 019 (1996)].

References

1 D. Bryce-Smith and A. Gilbert, *Tetrahedron*, 1976, **32**, 1309.
2 A. Gilbert, in *CRC Handbook of Organic Photochemistry and*

Photobiology, ed. W. M. Horspool and P-S. Song, CRC Press, Boca Raton, FL, 1995, ch. 18.
3 M. C. Sauer, A. D. Trifunac, D. B. McDonald and R. Cooper, *J. Phys. Chem.*, 1984, **88**, 4096.
4 A. Liu, M. C. Sauer and A. D. Trifunac, *J. Phys. Chem.*, 1994, **98**, 9546.
5 R. Srinivasan and A. P. Ghosh, *Chem. Phys. Lett.*, 1988, **143**, 546.
6 Y. Tsuboi, K. Hatanaka, H. Fukumura and H. Masuhara, *J. Phys. Chem.*, 1994, **98**, 11 237.
7 J. Singh, M. Vellaikal and J. Narayan, *J. Appl. Phys.*, 1993, **73**, 4351.
8 J. Pola, M. Urbanová, Z. Bastl, Z. Plzák, J. Šubrt, V. Vorlíček, I. Gregora, C. Crowley and R. Taylor, *Carbon*, 1997, **35**, 605.
9 S. E. Stein, *Carbon*, 1981, **19**, 421.
10 I. C. Lewis, *Carbon*, 1982, **20**, 519.
11 P. L. Walker, *Carbon*, 1990, **28**, 261.
12 Z. Plzák, M. Polanská and M. Suchánek, *J. Chromatogr. A*, 1995, **699**, 241.
13 J. R. Majer, *Adv. Fluorine Chem.*, 1961, **2**, 55.
14 W. J. Feast and W. E. Preston, *Tetrahedron*, 1972, **28**, 2805.
15 C-M. Hu, F. Long and Z-Q. Xu, *J. Fluorine Chem.*, 1990, **48**, 29.
16 J. L. Cotter, *J. Chem. Soc.*, 1965, 1520.
17 A. E. Hughes and B. A. Sexton, *J. Electron Spectrosc. Relat. Phenom.*, 1988, **46**, 31.
18 D. A. Shirley, *Phys. Rev. B*, 1972, **5**, 4709.
19 J. H. Scofield, *J. Electron Spectrosc. Relat. Phenom.*, 1976, **8**, 129.
20 G. Camaggi, F. Gozzo and G. J. Cevidalli, *Chem. Commun.*, 1966, 313.
21 I. Haller, *J. Am. Chem. Soc.*, 1966, **88**, 2070.
22 R. L. Whetten, K.-J. Fu, R. S. Tapper and E. R. Grant, *J. Phys. Chem.*, 1983, **87**, 1484.
23 E. N. Okafo and E. Whittle, *Int. J. Chem. Kinet.*, 1978, **10**, 591.
24 R. Gilbert and A. Theoret, *J. Phys. Chem.*, 1976, **80**, 1017.
25 M. J. Kroch, S. J. W. Price and W. F. Yared, *Can. J. Chem.*, 1974, **52**, 2673.
26 S. J. W. Price and H. Sapiano, *Can. J. Chem.*, 1974, **52**, 4109.
27 M. T. Duignan, E. Grunwald and S. Speiser, *J. Phys. Chem.*, 1983, **87**, 4387 and references therein.
28 H. Bürger and S. Sommer, *J. Chem. Soc., Chem. Commun.*, 1991, 456.
29 K. Sugawara, A. Watanabe, Y. Koga, H. Takeo, K. Fukuda, J. Hiraishi and C. Matsumura, *J. Phys. Chem.*, 1989, **93**, 3647.
30 A. Watanabe, Y. Koga, K. Sugawara, H. Takeo, K. Fukuda and C. Matsumura, *Spectrochim. Acta, Part A*, 1990, **46**, 463.
31 *NIST X-ray Photoelectron Spectroscopy Database*, US Dept. of Commerce, Gaithsburg, 1989.
32 D. Briggs and M. P. Seah, *Practical Surface Analysis*, Vol. 1, *Auger and Photoelectron Spectroscopy*, Wiley, Chichester, 1994, p. 622.
33 J. F. Moulder, W. F. Stickle, P. E. Sobol and K. D. Bomben, *Handbook of X-ray Photoelectron Spectroscopy*, ed. J. Chastain, Perkin Elmer Co., Physical Electronics Div., Eden Praire, MN, 1992, p. 234.
34 A. A. Galuska, H. H. Madenand and R. E. Allred, *Appl. Surf. Sci.*, 1988, **32**, 253.
35 J. M. Lascovich, R. Giorgi and S. Scaglione, *Appl. Surf. Sci.*, 1991, **47**, 17.
36 M. A. Tamor and W. C. Vassell, *J. Appl. Phys.*, 1994, **76**, 3823.
37 J. Wagner and P. Lautenschlager, *J. Appl. Phys.*, 1986, **59**, 2044.
38 R. d'Agostino, R. Lamendola, P. Favia and A. Giquel, *J. Vac. Sci. Technol. A*, 1994, **12**, 308.

Paper 7/03927A; *Received* 3rd *July*, 1997